# A novel control strategy for single-stage autotrophic nitrogen removal in SBR

Miguel Mauricio-Iglesias[a], Anna Katrine Vangsgaard[a], Krist V. Gernaey[a], Barth F. Smets[b] and Gürkan Sin[a,*]

[a]CAPEC-PROCESS, Department of Chemical and Biochemical Engineering, Technical University of Denmark, Building 229, Søltofts Plads, 2800 Lyngby, Denmark

[b]METlab, Department of Environmental Engineering, Technical University of Denmark, Building 115, Miljøvej 13, 2800 Lyngby, Denmark

***** Corresponding author. Tel.: +45 45252806; Fax: +45 45252906; E-mail: gsi@kt.dtu.dk

To be submitted to Chemical Engineering Journal

## Abstract

A novel feedforward-feedback control strategy was developed for complete autotrophic nitrogen removal in a sequencing batch reactor. The aim of the control system was to carry out the regulation of the process while keeping the system close to the optimal operation. The controller was designed based on a process model and then tested experimentally. The resulting batch-to-batch control strategy had the total nitrogen removal efficiency as controlled variable and the setting of the aeration mass flow controller as manipulated variable. Compared to manual operation mode (constant air supply), the controller resulted in a significant performance improvement: removal efficiency was kept at a stable high level in the presence of influent ammonium concentration disturbances,  and the absolute deviation on removal efficiency was reduced by 40%. The successful validation of the controller in a lab-scale reactor is a promising result, which brings this control strategy one step closer to full-scale implementation.



## Keywords

Autotrophic nitrogen removal; Sequencing batch reactor; Control design; Optimal operation; Experimental validation; Anammox

## 1 Nomenclature

| Abbreviation | Meaning | Unit (if relevant) |
|---|---|---|
| AE | Absolute error | (-) |
| AOB | Ammonium oxidizing bacteria | (-) |
| AnAOB | Anaerobic ammonium oxidizing bacteria (anammox bacteria) | (-) |
| CANR | Complete autotrophic nitrogen removal | (-) |
| DO | Dissolved oxygen | mg $O_2$ $L^{-1}$ |
| HB | Heterotrophic bacteria | (-) |
| i | Cycle number | (-) |
| $K_C$ | Proportional controller gain | mg $O_2$ / mg N |
| $K_{C,DO}$ | Proportional controller gain for the DO override loop | $d^{-1}$ (mg $O_2$ $L^{-1})^{-1}$ |
| $k_La$ | Volumetric mass transfer coefficient | $d^{-1}$ |
| $L_{NH4}$ | Volumetric ammonium loading rate | mg N $L^{-1}$ $d^{-1}$ |
| $L_{O2}$ | Volumetric oxygen loading rate | mg $O_2$ $L^{-1}$ $d^{-1}$ |
| MFC | Mass flow controller | (-) |
| $NH_4^+{}_{in}$ | Ammonium concentration in the influent | mg N $L^{-1}$ |
| $NH_4^+{}_{out}$ | Ammonium concentration in the effluent | mg N $L^{-1}$ |
| $NH_4^+{}_{start}$ | Ammonium concentration at the beginning of the SBR cycle | mg N $L^{-1}$ |
| $NO_2^-{}_{in}$ | Nitrite concentration in the influent | mg N $L^{-1}$ |
| $NO_2^-{}_{out}$ | Nitrite concentration in the effluent | mg N $L^{-1}$ |
| $NO_2^-{}_{start}$ | Nitrite concentration at the beginning of the SBR cycle | mg N $L^{-1}$ |
| $NO_3^-{}_{in}$ | Nitrate concentration in the influent | mg N $L^{-1}$ |
| $NO_3^-{}_{out}$ | Nitrate concentration in the effluent | mg N $L^{-1}$ |
| $NO_3^-{}_{start}$ | Nitrate concentration at the beginning of the SBR cycle | mg N $L^{-1}$ |
| NOB | Nitrite oxidizing bacteria | (-) |
| P | Proportional | (-) |
| PI | Proportional-integral | (-) |
| $Q_{air}$ | Air flow rate | L $min^{-1}$ |

| | | |
|---|---|---|
| $R_{AmmTot}$ | Ammonium removed over total nitrogen removed | mg N / mg N |
| $R_{AmmTot,sp}$ | Set point of ammonium removed over total nitrogen removed | mg N / mg N |
| RO | Ratio of volumetric oxygen loading rate over ammonium loading rate | mg $O_2$ / mg N |
| $RO_{sp}$ | Set point of volumetric oxygen loading rate over ammonium loading rate | mg $O_2$ / mg N |
| $RO_{sp,\infty}$ | Steady state set point of volumetric oxygen loading rate over ammonium loading rate | mg $O_2$ / mg N |
| ROC | RO controller | (-) |
| RRT | $R_{AmmTot}$ transmitter | (-) |
| RT | Total nitrogen removal efficiency – fraction | mg N / mg N |
| $RT_{sp}$ | Set point of total nitrogen removal efficiency | mg N / mg N |
| RTC | RT controller | (-) |
| $S_{O2,sat}$ | Oxygen saturation concentration | mg $O_2$ $L^{-1}$ |
| SBR | Sequencing batch reactor | (-) |
| $t_{aer}$ | Length of time that aeration is turned on during an SBR cycle | days |
| $t_{cycle}$ | Length of an entire SBR cycle | days |
| TN | Total nitrogen concentration | mg N $L^{-1}$ |
| $TN_{in}$ | Total nitrogen concentration in the influent | mg N $L^{-1}$ |
| VER | Volumetric exchange ratio | (-) |
| $\upsilon_s$ | Superficial gas flow velocity | m $s^{-1}$ |

# 1 Introduction

For wastewaters containing high amounts of nitrogen and low organic carbon to nitrogen ratios, complete autotrophic nitrogen removal (CANR) is a suitable, novel process that can increase the treatment capacity by increasing the volumetric removal rate by approximately five times compared to conventional nitrification-denitrification treatment. This process, originally designed as a two-stage SHARON-Anammox process [1], is convenient for treating anaerobic digester liquor, landfill leachate, or special industrial wastewaters, because costs related to the need of aeration and external carbon addition are lowered by 60% and 100%, respectively, compared to the conventional nitrification-denitrification treatment. The complete conversion of ammonium to nitrogen gas and a low amount of nitrate consists of a combination of two processes which are catalyzed by two different microbial groups that grow under different redox conditions, i.e. aerobic (AOB) and anaerobic (AnAOB) ammonium oxidizing bacteria. AOB oxidize ammonium to nitrite under aerobic conditions, while AnAOB oxidize the remaining ammonium using the nitrite produced by AOB as electron acceptor. Energy and capital costs can further be reduced by intensifying the process and performing it in a single biofilm reactor, where all processes take place simultaneously, e.g. in a granular sludge reactor. Here, the microbial groups can coexist, with the AOB growing in the outer oxygen-rich part of the granule and the AnAOB thriving in the interior anoxic parts. In addition, these two microbial groups are competing with other microbial groups, such as nitrite oxidizing bacteria (NOB) and heterotrophic bacteria (HB), resulting in a complex set of relationships among the microbial groups.

There is a general interest in reducing costs and improving efficiency during process operation. In this respect, the automatic control of bioreactors utilizing mixed cultures, such as the single-stage CANR, is important yet challenging given their highly nonlinear behavior, interactive dynamics, and frequent variations of the influent characteristics (flow rate, composition, temperature, etc.).

Furthermore, only a few actuators (e.g. base/acid addition, aeration, heating) are usually available to reject disturbances and maintain a stable operation, which is complicated due to competing microbial groups [2]. Operating a single-stage CANR system in a stable and efficient manner therefore requires an appropriate control strategy, which has typically been developed and operated through an experience-based approach [3].

In a previous contribution [4], we have shown how stoichiometric ratios between the different nitrogen species present in the CANR system are useful indicators of the operation state of CANR, including nitratation by NOB, the balance between AOB and AnAOB metabolism and nitrite accumulation. Likewise, it was indicated in Vangsgaard et al. [5] that the removal of ammonium to $N_2$ via partial nitritation and the anammox process can be maximized if the oxygen load is manipulated in accordance to the nitrogen load. These results allowed us to develop a controller for CANR in a continuous reactor, which was tested in a simulation study [2].

In this contribution, we have developed a novel control strategy for CANR in a sequencing batch reactor (SBR) and tested it experimentally at bench-scale. In order to implement the control system, i) a process model for the SBR operation was identified; ii) a control law was formulated that uses as inputs available measurements in the batch-to-batch SBR operation; and iii) the optimal set points for the controller were determined. The goal of the experimental testing of the controller was to validate the control strategy performance with respect to disturbance rejection in the form of varying ammonium loads. More specifically, disturbances in the influent ammonium were investigated, and the purpose of the controller was to maintain a stable (and efficient) performance of the nitrogen removal in the presence of such disturbances. The experiments consisted of subjecting the bench-scale reactor to designed perturbations in the operation while monitoring the resulting effect on the performance of the system.

This manuscript is organized as follows: First, the SBR setup is briefly described in the Materials and Methods section, and then the control strategy and the experimental planning for controller testing are described in a separate section. Experimental results are presented in the results section, and are followed by a discussion and conclusions.

# 2 Material and methods

## 2.1 Reactor features and operation

A bench-scale SBR, previously described in Vangsgaard et al. [6], was used for the experimental work. It has a volume of 4 L, was fed with synthetic wastewater with a default ammonium concentration of approximately 500 mg N $L^{-1}$ , and was operated in a sequential batch mode in cycles of 8 hours. The cycles consisted of a 10 minute fill phase, a 447 minute reaction phase, a 3 minute settling phase, a 10 minute draw phase, and a 10 minute idle phase. The volumetric exchange ratio (VER) was kept constant at 50%, which resulted in a volumetric loading rate of approximately 750 mg N $L^{-1}$ $d^{-1}$ (table 1).

At the time of testing, the reactor had been in manual operation for more than 2 years, with stable overall performance, and total N removal efficiencies exceeding 85% (Mutlu et al., in preparation). Quantification of the dominant functional guilds (AOB NOB, and AnAOB) based on nested quantitative 16S rRNA targeted PCR showed a slight dominance of AOB and AnAOB (1.5/1), with at least a 10 fold lower presence of NOB. The biomass was distributed over differently sized fractions (Mutlu et al., in preparation). In larger sized granules (90 μm < diameter < 600 μm), AnAOB dominated over AOB (ca.1.6/1 to 2/1), while in the smallest fractions (diameter < 90 μm), AOB dominated over AnAOB (up to 12/1).

### 2.2 Measurements and actuator

Effluent measurements of ammonium and nitrate were available on-line through ion selective electrodes (Varion, WTW, Weilheim, Germany), while the influent concentrations and the nitrite effluent concentration were measured by manual sampling and subsequent use of colorimetric test kit analyses (Merck KGaA, Darmstadt, Germany). The concentration of dissolved oxygen (DO) was measured by an OxyFerm FDA DO sensor (Hamilton, Bonaduz, Switzerland) and was available on-line during the reaction phase of the SBR cycle.

The controller actuator was the aeration flow ($Q_{air}$). In the physical setup, the air was supplied through a mass flow controller (EL-FLOW, Bronkhorst, Ruurlo, Netherlands). The setting of the mass flow controller (MFC) was therefore considered the actuator in the experimental laboratory implementation.

For the data acquisition and control purposes LabVIEW (National Instruments, Austin, TX, USA) was used, and the control algorithm was therefore also coded in a LabVIEW routine, which controlled the reactor operation.

# 3 Development of control structure

### 3.1 Definition of controller structure and control laws

The aim of the control strategy is to address both the regulation and the optimization of the operation, i.e. to ensure a stable operation and disturbance rejection while keeping the removal efficiency as high as possible. In a previous publication [5], it was seen that the maximum removal efficiency could be linked to the ratio between the oxygen and ammonium loading (RO). Based on this information, the control system is composed of two loops in cascade acting with different characteristic times. A fast feedforward loop adjusts the aeration flow depending on the ammonium load in the influent. As it will be seen later, the aeration flow can be related by a bijection to the volumetric mass transfer coefficient ($k_La$). Therefore, in a general formulation, the feedforward control law determining the $k_La$ can be expressed as follows:

$$k_L a = \frac{RO_{sp} NH^+_{4,in}}{HRT\left(S_{O2,sat}\right)} \quad (1)$$

where $RO_{sp}$ is the ammonium to oxygen loading set point, $NH^+_{4,in}$ is the ammonium concentration in the influent, HRT is the hydraulic retention time, and $S_{O2,sat}$ is the saturation concentration of oxygen.

A slower, feedback loop, corrects the set point value of the volumetric oxygen loading rate over ammonium loading rate ($RO_{sp}$) following a proportional control law:

$$RO_{sp} = \begin{cases} RO_{sp,\infty} - K_C * \left(RT_{sp} - RT\right), & R_{AmmTot} > R_{AmmTot,sp} \\ RO_{sp,\infty} + K_C * \left(RT_{sp} - RT\right), & R_{AmmTot} \le R_{AmmTot,sp} \end{cases} \quad (2)$$

In eq. 2, Kc stands for the magnitude of the gain of the master controller and its direction (sign) changes with the value of $R_{AmmTot}$. RT represents the ratio of total nitrogen removed over the total nitrogen in the influent and is a measurement of the efficiency of the process. $R_{AmmTot}$ is equal to the ammonium consumed per total nitrogen removed and can provide a measure of the relative activity of microbial groups present in the system, i.e. the AnAOB versus AOB and NOB activity.

$$RT = \frac{\Delta TN}{TN_{in}} = \frac{NH^+_{4,in} + NO^-_{2,in} + NO^-_{3,in} - NH^+_{4,out} - NO^-_{2,out} - NO^-_{3,out}}{NH^+_{4,in} + NO^-_{2,in} + NO^-_{3,in}} \quad (3)$$

$$R_{AmmTot} = \frac{\Delta NH^+_4}{\Delta TN} = \frac{NH^+_{4,in} - NH^+_{4,out}}{NH^+_{4,in} + NO^-_{2,in} + NO^-_{3,in} - NH^+_{4,out} - NO^-_{2,out} - NO^-_{3,out}} \quad (4)$$

In SBR systems, the measurements of the influent and the effluent wastewater composition are typically only available once per cycle, and the nature of the operation is discontinuous. Hence, a batch-to-batch type controller was formulated, in which the feedback was provided after the conclusion of a batch cycle, and the feedforward was active once per cycle during the fill phase, when the influent was pumped to the reactor (Figure 1). Such a procedure to reconcile the measurements from different batches to provide feedback and feedforward action can also be extended to other SBRs. In this case, the control law was therefore computed once per cycle, which provided the signal for the aeration (i.e. the MFC value) implemented by the controller.

For a SBR, the magnitudes appearing in the control equations were defined as follows. The volumetric oxygen loading to the system ($L_{O2}$) during one cycle was calculated as:

$$L_{O2,i} = k_L a_i \cdot S_{O2,sat} \frac{t_{aer,i}}{t_{cycle,i}} \tag{5}$$

where the subscript i denotes the number of the cycle, $t_{aer,i}$ is the duration of the period where aeration is turned on during cycle i, and $t_{cycle,i}$ is the length of the entire cycle i.

Similarly, the volumetric ammonium loading rate was defined as:

$$L_{NH4,i} = \frac{NH^+_{4,in,i} VER + NH^+_{4,out,i-1}\left(1 - VER\right)}{t_{cycle,i}} \tag{6}$$

where $NH^+_{4,in,i}$ represents the ammonium concentration of the influent being pumped in during the fill phase of cycle i, VER is the volumetric exchange ratio, defined as the volume leaving the reactor at the end of the cycle divided by the entire volume of the reactor when full, and $NH^+_{4,out,i-1}$ is the effluent concentration of the cycle before cycle i, i.e. cycle i-1.

The oxygen to ammonium loading rate ratio can therefore be defined as:

$$RO_i = \frac{k_L a_i S_{sat,O2} t_{aer,i}}{\left(NH^+_{4,in,i} ER + NH^+_{4,out,i-1}\left(1 - VER\right)\right)} \quad (7)$$

Finally, the feedforward control law (eq. 1) becomes:

$$k_L a_i = \frac{RO_{sp,i}\left(NH^+_{4,in,i} VER + NH^+_{4,out,i-1}\left(1 - VER\right)\right)}{S_{sat,O2} t_{aer,i}} \quad (8)$$

The removal efficiency was calculated as specified below. Since the value was updated once per cycle, the following expression was obtained:

$$RT_i = \frac{\Delta TN_i}{TN_{in,i}} = \frac{NH^+_{4,in,i} + NO^-_{2,in,i} + NO^-_{3,in,i} - NH^+_{4,out,i} - NO^-_{2,out,i} - NO^-_{3,out,i}}{NH^+_{4,in,i} + NO^-_{2,in,i} + NO^-_{3,in,i}} \quad (9)$$

$R_{AmmTot}$, the metric capturing the relative activity of the microbial groups, was defined as:

$$R_{AmmTot,i} = \frac{NH^+_{4,start,i} - NH^+_{4,out,i}}{TN_{start,i} - TN_{out,i}} = \frac{\left(NH^+_{4,in,i} VER + NH^+_{4,out,i-1}(1 - VER)\right) - NH^+_{4,out,i}}{\left(\left(NH^+_{4,in,i} + NO^-_{2,in,i} + NO^-_{3,in,i}\right) VER + \left(NH^+_{4,out,i-1} + NO^-_{2,out,i-1} + NO^-_{3,out,i-1}\right)(1 - VER)\right) - NH^+_{4,out,i} - NO^-_{2,out,i} - NO^-_{3,out,i}} \quad (10)$$

The feedback control law, correcting the oxygen to ammonium loading rate ratio, takes the removal efficiency and the $R_{AmmTot}$ value from the previous cycle into account:

$$RO_{sp,i+1} = \begin{cases} RO_{sp,\infty} - K_C * \left(RT_{sp} - RT_i\right), & R_{AmmTot,i} > R_{AmmTot,sp} \\ RO_{sp,\infty} + K_C * \left(RT_{sp} - RT_i\right), & R_{AmmTot,i} \le R_{AmmTot,sp} \end{cases} \quad (11)$$

The value of the proportional gain was selected as the inverse of the process gain between the manipulated variable (RO) and the controlled variable (RT). Simulations of step changes of the $k_La$ value in the SBR system, with the model described in Vangsgaard et al. [5], provided a value of 2 (mg $O_2$ $L^{-1}$ $d^{-1}$)/(mg N $L^{-1}$ $d^{-1}$) for the ratio $|\Delta RO/\Delta RT|$. Hence, this value relates the manipulated and the controlled variable and can be seen as the process gain for the feedback loop.

The control structure, and the relation between the cycle number, data acquisition and controller action can be seen in Figure 1.

<Figure 1 should be placed here>

In the control algorithm presented above an override loop for DO was implemented during SBR operation as follows:

$$k_La = \begin{cases} k_La & DO < 0.2 \text{ mg } O_2 L^{-1} \\ k_La - K_{C,DO}\left(DO - 0.2\right) & DO \geq 0.2 \text{ mg } O_2 L^{-1} \end{cases} \quad (12)$$

This extra loop ensured that the aeration intensity was decreased in case the DO rose above 0.2 mg $O_2$ $L^{-1}$ in the bulk liquid. The value of $K_{C,DO}$ was set to 130 $d^{-1}$ (mg $O_2$ $L^{-1}$)$^{-1}$ so that the aeration was reduced if DO rose above 0.2 mg $O_2$ $L^{-1}$. Since the $k_La$ fluctuated around 150 $d^{-1}$, the aeration would stop completely at a DO of approximately 1.3 mg $O_2$ $L^{-1}$. In rare cases where the DO rises excessively, the outcome of eq. 12 can be negative $k_La$ values which were of course set equal to zero, meaning a complete stop of the aeration. Since the influent ammonium and effluent nitrite concentrations were measured manually, their values were updated for two out of the three 8 hour cycles per day. For the third cycle, during the night, the values obtained from the second cycle of the day were used. The effluent ammonium and nitrate concentrations were updated every cycle, because they were continuously logged on-line.

### 3.2. Calibration of aeration flow and $k_La$ value

From the control laws presented above, a $k_La$ value was obtained. This value then had to be translated to a valve setting, in percent, for the mass flow controller (MFC) which was the actuator available in the experimental setup. For a broad range of operation conditions, the relationship between $k_La$ and air flow rate ($Q_{air}$) is not necessarily linear and must be calibrated [7]. The following shows how the relationship between $k_La$ and the valve setting in the MFC was characterized.

First, an empirical correlation was used to check the relation between the air flow rate and the oxygen mass transfer coefficient. One can find a large number of correlations that relate stirring, aeration and $k_La$ in stirred tank reactors. In general, most are variations or refinements of this general equation [8]:

$$k_L a = 0.026\left(\frac{P}{V}\right)^{0.4} \upsilon_s^{0.5} \qquad (13)$$

where $\upsilon_s$ is the superficial gas velocity and (P/V) is the power to volume number; here, P is the power dissipated under aeration conditions (W) and V is the volume of liquid in the reactor ($m^3$). Far from the gas-flooding region, both P/V and $\upsilon_s$ are proportional to the air flow rate ($Q_{air}$), which results in $k_La$ being proportional to $Q_{air}^{0.9}$, which is close to a linear relationship. The experimental data confirmed these predictions: within the air flow range used in the reactor operation and for constant stirring rate, the relation was regressed to a linear equation with a high correlation coefficient, as follows:

$$Q_{air} = 0.0022\ k_La \qquad R^2=0.98 \qquad (14)$$

with $Q_{air}$ in L $min^{-1}$ and $k_La$ in $d^{-1}$. The next step was to relate the air flow rate to the setting of the mass flow controller. This was done through an experimental calibration, where two ranges were identified, an upper range and a lower range. A piece-wise linear relation consisting of two linear ranges was established:

$$Q_{air} = 0.0351\ MFC_{sp} + 0.0241 \qquad R^2=0.997 \qquad \text{for } MFC_{sp} < 25\% \qquad (15a)$$

$$Q_{air} = 0.0168\ MFC_{sp} + 0.556 \qquad R^2=0.994 \qquad \text{for } 25\% < MFC_{sp} < 50\% \qquad (15b)$$

where $Q_{air}$ is in L $min^{-1}$ and $MFC_{sp}$ is the setting of the mass flow controller (in % of maximum). Combining eq. 14 with eq. 15, a relationship between $k_La$ and the MFC setting can be established.

## 3.3 Experiments for testing control performance

### *Performance during set point change*

In order to first check that the ability of the controller to track a set point, starting from an $RT_{sp}$ set point of 0.925, a set point change was imposed in which $RT_{sp}$ was set to 0.7 for a period of 8 days. Afterwards, a set point increase back to $RT_{sp}$ = 0.925 was employed to restore the original performance of the system. During the set point change experiment $t_{aer}$ was 390 minutes, compared to a value of 447 minutes for the overall reaction phase. The aeration time was distributed over three aerated phases of 130 minutes each.

### *Performance during disturbance in feed*

Feed concentration disturbances were introduced by imposing a square wave signal, i.e. an ammonium concentration increase for a number of cycles followed by a decrease back to the original concentration level. One experiment was conducted with the manual operation mode (actuator at a fixed value) and one experiment was conducted with the controller active (i.e. in automatic mode). When applying the square wave, the ammonium concentration was increased by approximately 20%, i.e. from around 500 mg N $L^{-1}$ to around 600 mg N $L^{-1}$. This increase lasted for one day, i.e. during three SBR cycles. In this case, the reactor was continuously aerated during the reaction phase, which resulted in $t_{aer}$= 447 minutes.

### *Performance during dynamic influent profile*

A dynamic influent profile was imposed to the system during five days, in which the influent concentration ranged between approximately 400 mg N $L^{-1}$ and 700 mg N $L^{-1}$. When applying the dynamic influent profile, the influent concentration was changed once per day (Figure 2). After imposing these disturbances in the feed, the influent ammonium concentration was restored to a level around 500 mg N $L^{-1}$, and the reactor was operated with this constant influent for 10 days in order to allow a more long-term monitoring of the system performance. As in the feed disturbance experiment, the reaction phase was continuously aerated during the dynamic influent experiment, such that $t_{aer}$= 447 minutes.

<Figure 2 should be placed here>

### *Determination of controller set points*

During all experiments, $R_{AmmTot,sp}$ = 1.15 was used. This value was obtained from long-term observation of the lab-scale reactor prior to the start of the controller validation experiments. The steady state set point value of the oxygen to ammonium loading ratio was found through simulation studies to be $RO_{sp,\infty}$ = 1.67 (mg $O_2$ $L^{-1}$ $d^{-1}$)/(mg N $L^{-1}$ $d^{-1}$). During the disturbance introduction experiments $RT_{sp}$ = 0.925 was used; however this value was readjusted to 0.90 during the dynamic influent profile experiment on the basis of experimental observations showing that the maximum removal efficiency produced by the system never reached higher than 0.90.

# 4 Results and discussion

## 4.1 Set point change response

The performance of the reactor was relatively stable before the implementation and testing of the controller (Figure 3). In order to test the impact of the controller a set point tracking experiment was conducted. At day 2 of this experiment the controller was implemented, and the performance dropped to a lower level where it stabilized within 1-2 days (Figure 3). The set point was increased on day 10 of the experiment, and, apart from a single point accounted for by an operational upset due to a pump failure on day 11, the performance went back up to the initial level of around 89% removal within one day.

However, when the low set point of $RT_{sp}$ = 0.7 was used, the offset from the set point was still rather significant. The controller was retuned by increasing the controller gain ($K_C$), first from 2 to 3 (mg $O_2$ $L^{-1}$ $d^{-1}$)/(mg N $L^{-1}$ $d^{-1}$) and later from 3 to 4 (mg $O_2$ $L^{-1}$ $d^{-1}$)/(mg N $L^{-1}$ $d^{-1}$). Subsequently, the performance leveled off at a total nitrogen (TN) removal of 82%, which showed an offset from the set point of 70%, but still showed a significant change in the performance from the manual operation achieved before the controller implementation (Figure 3). The significant offset from the set point was caused by the proportional-only control law – a known deficiency of a proportional-only controller–, which results in a significant steady state error related to the controller gain [9].

<Figure 3 should be placed here>

## 4.2 Responses to influent ammonium disturbances

During the manual operation (the MFC in manual mode at a fixed value), it was observed that the increase in ammonium concentration in the influent propagated to the effluent (Figure 4, top).

Concurrently, the nitrate concentration dropped slightly. In the controlled case (MFC in automatic mode) the ammonium concentration remained low throughout the experiment, but the nitrite concentration increased slightly and varied between 0 and 10 mg N $L^{-1}$ (Figure 4, top). The fluctuations in effluent concentrations were reflected in the larger offset in the removal efficiency in the manual operation mode than when the controller was set to automatic (Figure 4, bottom). The absolute error (AE) defined as:

$$AE = \sum_{1}^{n_{cycle}} \left( RT_{sp} - RT \right) \quad (16)$$

where RT is the measured removal efficiency.

The AE went from 0.98 in the manual operation mode to 0.59 in automatic mode, and thus a 40% reduction in the absolute error was obtained.

In automatic mode, it was observed that the MFC set point decreased when the value of $R_{AmmTot}$ exceeded its set point value, e.g. in cycle two and eight, counting from the start of the experiment. Finally, the role of the DO override loop could also be observed in the end of the second cycle. The MFC value decreased suddenly (Figure 4, bottom), because the DO concentration went above 0.2 mg $O_2$ $L^{-1}$. The rapid rise in DO was followed by a very low (practically zero) effluent ammonium concentration, suggesting that the DO increase was due to oxidation of all ammonium present before the end of the reaction phase.

<Figure 4 should be placed here>

### 4.3 Dynamic influent response

In order to test the stability and long-term effects and impacts of the control strategy, a dynamic influent profile was imposed to the reactor: the reactor was switched to automatic mode, and subsequently observed for 15 days.

The results showed that the removal efficiency was not optimal in the beginning of the experiment, with residual ammonium remaining in the effluent (Figure 5, middle). This effluent ammonium concentration was quickly reduced despite the fluctuations in the influent concentration, thus demonstrating that the controller could rapidly produce a good and stable effluent quality under varying load conditions. At day 4 of the experiment, the influent concentration increased to 735 mg N $L^{-1}$, which resulted in an increase in the ammonium effluent concentration. Subsequently, the nitrite concentration increased and fluctuated between 5 and 45 mg N $L^{-1}$ for the following 3-4 days. During this time the nitrate concentration reached a lower level than in the beginning of the experiment and after this period it increased slightly again.

As a consequence of, mainly, the effluent concentration variations, the total nitrogen removal efficiency (RT) dropped at day 4 of the experiment (Figure 5, bottom). Since both ammonium and nitrite were present in the effluent, it could be deduced that AnAOB activity was not sufficient to keep a high removal efficiency. There could be two reasons for this behavior: 1) The maximum capacity of the sludge present in the reactor was reached, and the biomass did not have enough time to grow during the testing period to produce sufficient biomass to convert all ammonium and nitrite present; or, 2) due to the higher oxygen supply compared to nominal conditions (Figure 5 top), the AnAOB were oxygen inhibited to some extent, despite the fact that the DO bulk level never reached detectable concentrations during this part of the experiment, since studies have shown AnAOB inhibition at dissolved oxygen concentrations as low as 0.2 mg $O_2$ $L^{-1}$ [10]. From these results, it cannot be deduced whether it was insufficient AnAOB capacity, AnAOB inhibition, or a combination of the two, which was responsible for the observed efficiency decrease.

Despite the drop in removal efficiency on day 4 of the experiment, the total nitrogen removal rate (in mg N $L^{-1}$ $d^{-1}$) was higher at this point of the experiment than previously due to the higher total nitrogen loading rate (Figure 5, top).

The oscillations in nitrite concentrations from day 4 to 8 of the experiment initiated oscillations in $R_{AmmTot}$ around the set point value (Figure 5, bottom), which in turn caused oscillations in the set point of the actuator (the MFC set point which varied from cycle to cycle). These oscillations were reflected (Figure 5, top) in the oxygen to ammonium loading ratio (RO) and in the oxygen loading rate ($L_{O2}$).

<Figure 5 should be placed here>

As a consequence of this oscillatory behavior and the relatively low removal efficiency, the controller was retuned at day 7 of the experiment, by decreasing the proportional gain ($K_C$) from 4 back down to 3 (mg $O_2$ $L^{-1}$ $d^{-1}$)/(mg N $L^{-1}$ $d^{-1}$), which was also closer to the gain of 2 (mg $O_2$ $L^{-1}$ $d^{-1}$)/(mg N $L^{-1}$ $d^{-1}$) found when tuning on the basis of the step input simulation data (section 3.1). After this point, the oscillations dampened and the performance again reached a high and stable level (Figure 5).

## 4.4 Comparison of experimental and simulated results

Qualitatively, similar trends can be observed when comparing the experimental results from the influent ammonium concentration perturbations – both with the controller and with the manual operation mode (Figure 4) – and the simulation results (Figure 6) of the same square wave signal influent profile.

Figure 6 should be placed here>

However, from the deviations between experiments and simulation results, it can be observed that the response in the ammonium effluent concentration, and hence also the response in removal efficiency, in manual operation, was faster in simulation (Figure 6) than in the experimental observations (Figure 4). The difference in time response led us to hypothesize that there might be a practical time delay, which is not included in the model, e.g. caused by probe response time or due to a lag time in response of bacterial activity, especially when exposed to periodically changing operating conditions, like in the SBR operation or during intermittent aeration, which has been observed frequently elsewhere [11-13]. Including such transient response phenomena in the model is therefore expected to result in a better agreement between experiments and simulations [14], and will thus further refine the quality of the model.

Secondly, a difference in the level of the nitrate concentration could be observed, where the experimental observations were higher than the simulation results. This is likely due to the estimated heterotrophic denitrification rate being higher in simulation than in the reactor during the experiments. The lower amount of HB activity also affects the values of $RT_{sp}$ and $R_{AmmTot,sp}$, which were, precisely for this reason, based on experimental observations from about a month before the start of the experiments, instead of directly based on the values obtained from simulation.

The steady state offset observed during the set point change was higher than expected from model simulations, which indicates a certain model mismatch as addressed above. One way to handle this difference and to overcome an undesired large offset could be to implement an integral term in the feedback loop, instead of having a purely proportional feedback action. The proportional controller was deemed sufficient in this case, because offsets from the removal efficiency set point could be tolerated. In effect, the effluent from reactors using this technology is most often recycled back to the main-stream treatment and not directly discharged, thus not constrained by strict discharge limits.

### 4.5 Perspectives on transfer of the control technology to industrial practice

From the experience obtained in this work, it is believed that the control strategy can also be implemented during a startup of nitritation-anammox reactors. Additionally, the ammonium loading to the system is also often controlled during startups [15] and gradually ramped up as the concentrations of the microbial groups slowly increase to the desired levels [16]. As the ammonium loading is an input to the feedforward controller, providing information about the ammonium loading ramp will ensure that the appropriate amount of oxygen is supplied to the system along the startup.

Improvements to the current technology would include a more frequent update of measurements. In effect, influent ammonium and effluent nitrite concentration values were only updated (manually) for two out of three cycles. In cases where the nitrite concentration varied from cycle to cycle, only updating the controller two out of three times did not help to decrease the oscillatory behavior (Figure 5). On-line measurements of nitrite, e.g. from on-line UV light absorption measurements [17] or by ion selective electrodes [18] are expected to improve the controller performance. It was also observed that the established relationship between the $k_La$ and the value of the MFC setting (the actuator of the physical equipment) has a considerable impact on the MFC setting value obtained from the controller. Calibrating this curve should therefore be done on a frequent basis, and a detailed knowledge of this relationship every time a new system is started up is definitely a necessity.

As observed during the set point change experiment, a higher gain resulted in a smaller offset from the set point without resulting in instability and oscillatory behavior. However, as seen in cases of system capacity limitation (high concentrations during the dynamic influent experiment), the system was very sensitive towards the gain value of the proportional feedback control loop, in particular when operating at high removal efficiencies. Gain scheduling could therefore be an alternative idea to add to the control technology [9]. The implementation could be done by defining a metric (error signal), which gives information about the distance between the current state of the system and its capacity limit. Based on this information, the gain value would change accordingly. In other words, the further the current operation is from the capacity limit, the higher the gain should be since the process is far from the limits.

Finally, it should also be mentioned, that the control strategy validated in this study was a single-loop controller considering one actuator. Possibilities of extending it to a multi-loop strategy include utilizing the pH level to control the exchange ratio or to control the length of the SBR cycle, similarly to the study by [19], by which the volumetric removal rate might be improved due to higher loading rates. The pH signal has previously been used to control the nitritation process [20] and a single-stage nitritation-anammox process [21]. Experimental work (results not shown) has demonstrated that the pH signal often responded faster than the DO signal, in cases of ammonium depletion before the end of the reaction phase. It is therefore believed that utilizing this measurement as well could further optimize the reactor performance.

In summary, while there is room for further refinement and polishing, as mentioned above, the evidence from experimental testing certainly demonstrates promising potential of this control technology for full-scale operation of autotrophic nitrogen removal in an SBR configuration. The originality of the control strategy lies in the fact that it is the first time that a process performance (in this case nitrogen removal efficiency) is directly linked to a control objective function, translated to a set point for the regulatory layer, and finally experimentally verified.

# 5 Conclusions

A novel batch-to-batch control strategy for a single-stage CANR process was developed, tested, and validated in a bench-scale SBR. From the experimental results it can be concluded that:

- The controller successfully rejected the influent disturbances and maintained high removal efficiency.
- Qualitatively similar results were obtained when comparing the simulation based controller testing and the experimental testing, highlighting the importance of model-based tests for controller development prior to implementation.
- Incremental refinement of the controller (retuning) during experimental testing was needed to avoid oscillatory behavior during high ammonium loading rates.

Further improvements include the utilization of additional measurements for development of multi-loop strategies.

**Acknowledgements**

This research is funded, in part, by the Danish Agency for Science, Technology and Innovation through the Research Centre for Design of Microbial Communities in Membrane Bioreactors (09-067230).

# 6 References


[1] van Dongen, U.G.J.M., Jetten, M.S.M., van Loosdrecht, M.C.M., 2001. The SHARON-Anammox process for treatment of ammonium rich wastewater. Water Sci Technol **44**(1), 153-160.

[2] Vangsgaard, A.K., Mauricio-Iglesias, M., Gernaey, K.V., Sin, G., 2014. Development of novel control strategies for single-stage autotrophic nitrogen removal: A process oriented approach. Comp Chem Eng **66**, 71–81

[3] Vlaeminck, S.E., De Clippeleir, H., Verstraete, W., 2012. Microbial resource management of one-stage partial nitritation/anammox. Microbial Biotechnol **5**(3), 433-448.

[4] Mutlu, A.G., Vangsgaard, A.K., Sin, G., Smets, B.F., 2013. An operation protocol for facilitating start-up of single-stage autotrophic nitrogen removing reactors based on process stoichiometry. Water Sci Technol **68**(3), 514-521.

[5] Vangsgaard, A.K., Mauricio-Iglesias, M., Gernaey, K.V., Smets, B.F., Sin, G., 2012. Sensitivity analysis of autotrophic N removal by a granule based bioreactor: Influence of mass transfer versus microbial kinetics. Bioresource Technol **123**, 230-241.

[6] Vangsgaard, A.K., Mutlu, A.G., Gernaey, K.V., Smets, B.F., Sin, G., 2013. Calibration and validation of a model describing complete autotrophic nitrogen removal in a granular SBR system. J Chem Technol Biotechnol **88** (11), 2007-2015

[7] Åmand, L., Olsson, G., Carlsson, B., 2013. Aeration control – a review. Water Sci Technol **67**(11), 2374-2398.

[8] Van't Riet, K., 1979. Review of Measuring Methods and Results in Nonviscous Gas-Liquid Mass Transfer in Stirred Vessels. Ind Eng Chem Process Des Dev **18**(3), 357-364.

[9] Seborg, D.E., Edgar, T.F., Mellichamp, D.A., 2004. Process Dynamics and Control. Second edition, John Wiley & Sons Inc.

[10] Jung, J.Y., Kang, S.H., Chung, Y.C., Ahn, D.H., 2007. Factors affecting the activity of anammox bacteria during start up in the continuous culture reactor. Water Sci Technol **55**(1-2), 459-468.

[11] Katsogiannis, A.N., Kornaros, M., Lyberatos, G., 2003. Enhanced nitrogen removal in SBRs bypassing nitrate generation accomplished by multiple aerobic/anoxic phase pairs. Water Sci Technol **47**(11), 53-59.

[12] Zhang, M., Lawlor, P.G., Wu, G., Lynch, B., Zhan, X., 2011. Partial nitrification and nutrient removal in intermittently aerated sequencing batch reactors treating separated digestate liquid after anaerobic digestion of pig manure. Bioproc Biosyst Eng **34**(9), 1049-1056.

[13] Wett, B., Omari, A., Podmirseg, S.M., Han, M., Akintayo, O., Gómez Brandón, M., Murthy, S., Bott, C., Hell, M., Takács, I., Nyhuis, G., O'Shaughnessy, M., 2013. Going for mainstream deammonification from bench to full scale for maximized resource efficiency. Water Sci Technol **68**(2), 283-289.

[14] Vanrolleghem, P.A., Sin, G., Gernaey, K.V., 2004. Transient Response of Aerobic and Anoxic Activated Sludge Activities to Sudden Substrate Concentration Changes. Biotechnol Bioeng **86**(3), 277-290.

[15] Christensson, M., Ekström, S., Andersson Chan, A., Le Vaillant, E., Lemaire, R., 2013. Experience from start-up of the first ANITA Mox Plants. Water Sci Technol **67**(12), 2677-2684.

[16] van der Star, W.R.L., Abma, W.R., Blommers, D., Mulder, J.W., Tokutomi, T., Strous, M., Picioreanu, C., van Loosdrecht, M.C.M., 2007. Startup of reactors for anoxic ammonium

oxidation: Experiences from the first full-scale anammox reactor in Rotterdam. Water Res **41**(18), 4149-4163.

[17] Rieger, L., Langergraber, G., Thomann, M., Fleischmann, N., Siegrist, H., 2004. Spectral in-situ analysis of NO2, NO3, COD, DOC and TSS in the effluent of a WWTP. Water Sci Technol **50**(11), 143-152.

[18] Kaelin, D., Rieger, L., Eugster, J., Rottermann, K., Bänninger, C., Siegrist, H., 2008. Potential of in-situ sensors with ion-selective electrodes for aeration control at wastewater treatment plants. Water Sci Technol **58**(3), 629-637.

[19] Lemaire, R., Marcelino, M., Yuan, Z., 2008. Achieving the nitrite pathway using aeration phase length control and step-feed in an SBR removing nutrients from Abattoir wastewater. Biotechnol Bioeng **100**(6), 1228-1236.

[20] Volcke, E.I.P., van Loosdrecht, M.C.M., Vanrolleghem, P.A., 2006. Controlling the nitrite:ammonium ratio in a SHARON reactor in view of its coupling with an Anammox process. Water Sci Technol **53**(4-5), 45-54.

[21] Wett, B., 2007. Development and implementation of a robust deammonification process. Water Sci Technol **56**(7), 81-88.

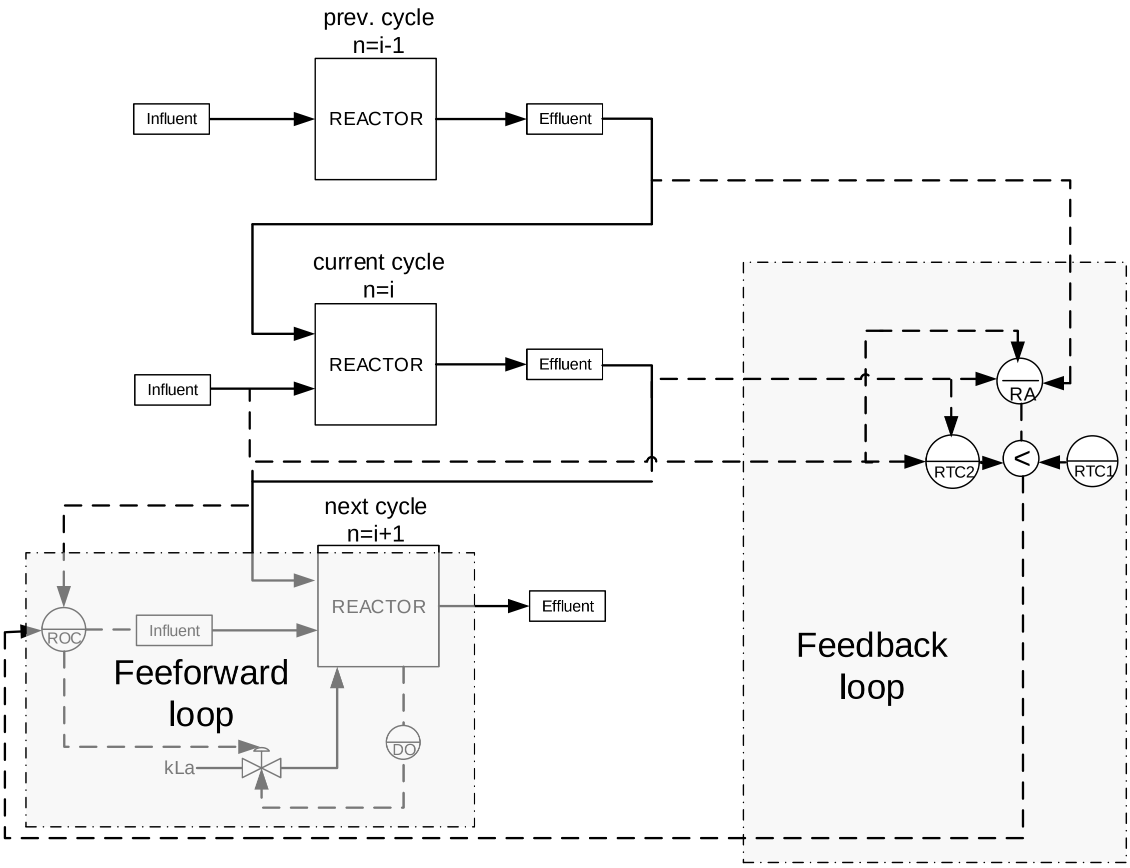


**Figure 1** Structure of the controller. n is the cycle number, RA is the $R_{AmmTot}$ transmitter, RTC1 and RTC2 are the removal efficiency controllers (1 indicating a positive control action and 2 indicating a negative control action), and ROC is the oxygen to ammonium loading ratio controller.

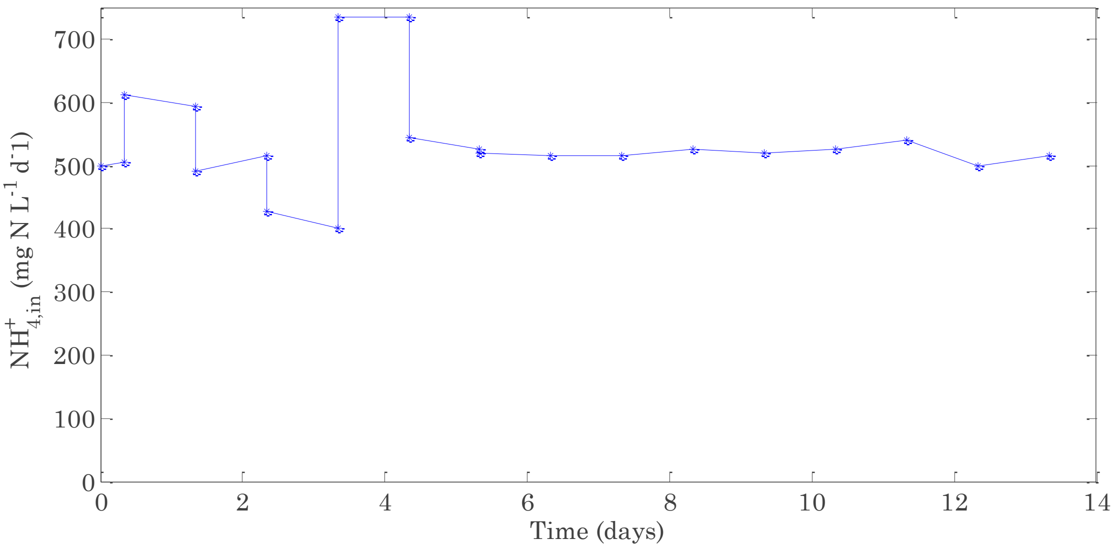


**Figure 2** Dynamic influent concentration profile for long term disturbance rejection experiments

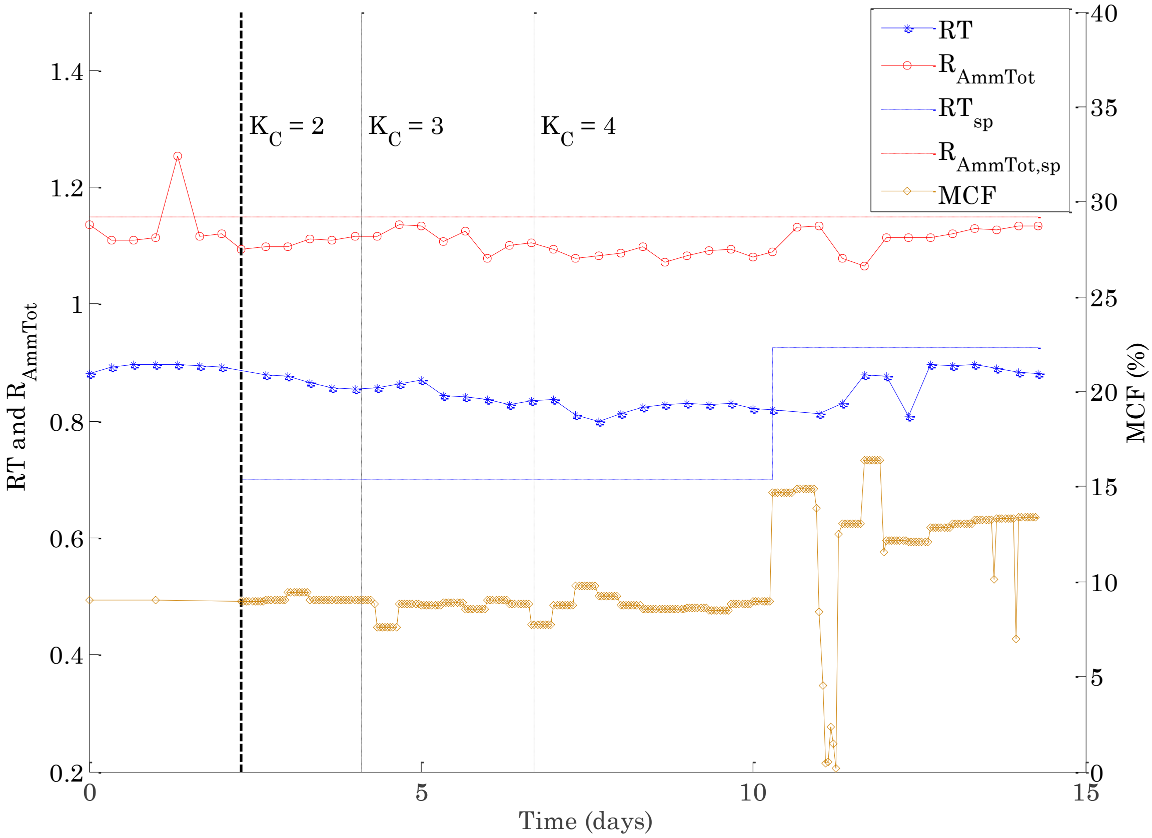


**Figure 3** Set point change experiment. Evolution of controlled and manipulated variables as a function of time. The vertical dashed black line indicates the transition from manual to automatic mode. The vertical dash-dotted lines indicate the fine-tuning of the controller gain.

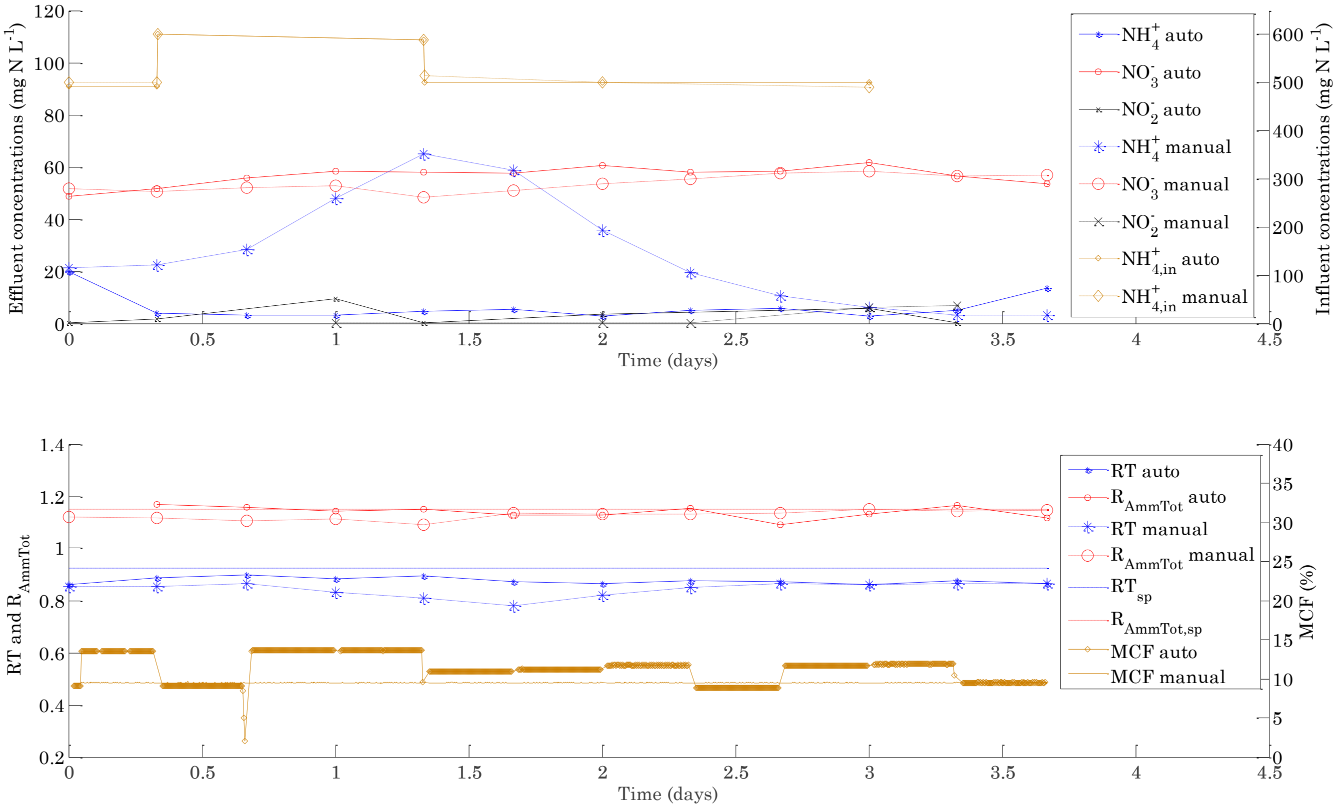


**Figure 4** Top: Influent and effluent concentrations during the feed disturbance experiment. Bottom: Evolution of the controlled and manipulated variables as a function of time. Full lines: Experiments in automatic mode (auto in the legend). Dashed line: Experiments in manual mode

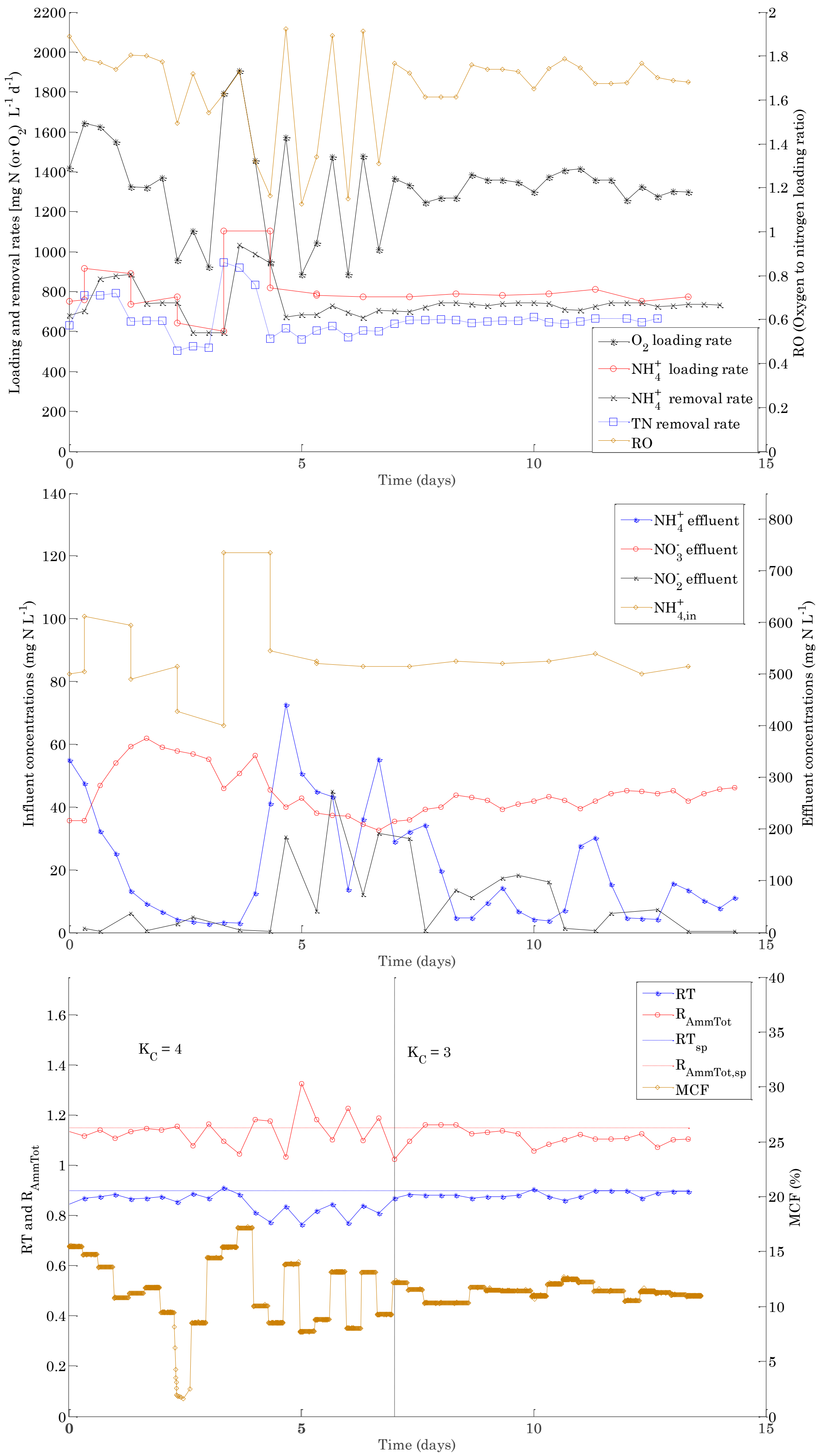
Loading and removal rates [mg N (or O2) L-1 d-1)
RO (Oxygen to nitrogen loading ratio)
O2 loading rate
NH4+ loading rate
NH4+ removal rate
TN removal rate
RO
Time (days)
Influent concentrations (mg N L-1)
Effluent concentrations (mg N L-1)
NH4+ effluent
NO3- effluent
NO2- effluent
NH4,in+
Time (days)
RT and RAmmTot
MCF (%)
KC = 4
KC = 3
RT
RAmmTot
RTsp
RAmmTot,sp
MCF
Time (days)

**Figure 5** Time evolution of the dynamic influent experiment. On day 7 the gain was decreased by 25%. Top: Ammonium and oxygen volumetric loading rates (RO), and ammonium and total nitrogen removal rate. Middle: Influent and effluent concentrations. Bottom: Evolution of controlled and manipulated variables.

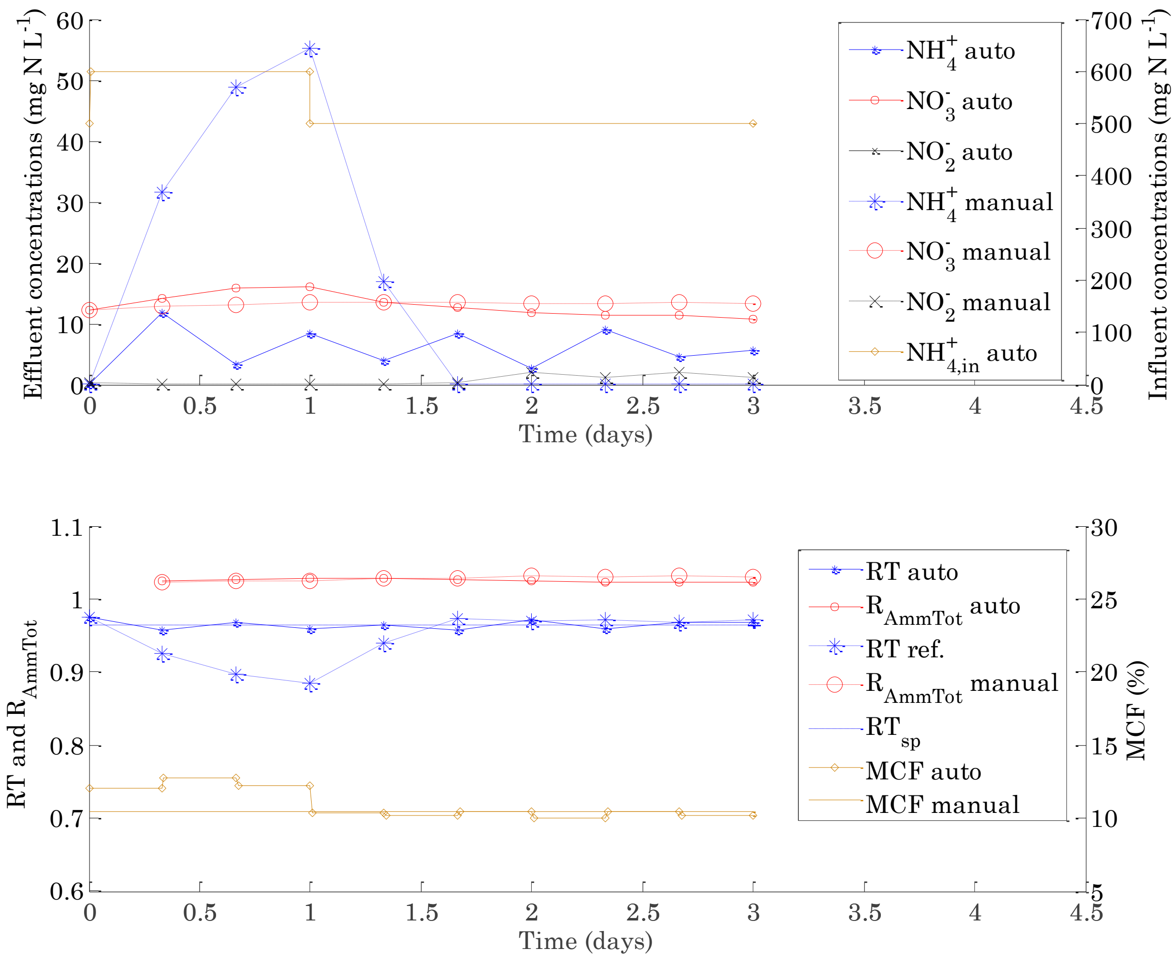


**Figure 6** Top: Simulation results showing influent and effluent concentrations during a feed disturbance experiment. Bottom: Simulation results of the controlled and manipulated variables matching the influent disturbance introduction.

Table 1. Influent and operational characteristics

| | |
|---|---|
| Reactor volume | 4 L |
| Cycle length | 8 h |
| Volumetric exchange ratio | 50% |
| Ammonium concentration | 500 mg N $L^{-1}$ |
| Ammonium loading rate | 750 mg N $L^{-1}$ $d^{-1}$ |